



**HAL**  
open science

## Experimental characterisation of macro-crack propagation in 3D woven composites, size effect and associated damage gradient models

Victor Médeau, Frédéric Laurin, Johann Rannou, Antoine Hurmane, S Mousillat, Frederic Lachaud

### ► To cite this version:

Victor Médeau, Frédéric Laurin, Johann Rannou, Antoine Hurmane, S Mousillat, et al.. Experimental characterisation of macro-crack propagation in 3D woven composites, size effect and associated damage gradient models. ECCM18 – 18th European Conference on Composite Materials, Jun 2018, Athens, Greece. hal-03189106

**HAL Id: hal-03189106**

**<https://hal.science/hal-03189106v1>**

Submitted on 2 Apr 2021

**HAL** is a multi-disciplinary open access archive for the deposit and dissemination of scientific research documents, whether they are published or not. The documents may come from teaching and research institutions in France or abroad, or from public or private research centers.

L'archive ouverte pluridisciplinaire **HAL**, est destinée au dépôt et à la diffusion de documents scientifiques de niveau recherche, publiés ou non, émanant des établissements d'enseignement et de recherche français ou étrangers, des laboratoires publics ou privés.

# EXPERIMENTAL CHARACTERISATION OF MACRO-CRACK PROPAGATION IN 3D WOVEN COMPOSITES, SIZE EFFECT AND ASSOCIATED DAMAGE GRADIENT MODELS

V. MÉDEAU<sup>1,2,3</sup>, F. LAURIN<sup>1</sup>, J. RANNOU<sup>1</sup>, A. HURMANE<sup>1</sup>  
S. MOUSILLAT<sup>2</sup> and F. LACHAUD<sup>3</sup>

<sup>1</sup>ONERA, DMAS, Université Paris Saclay, F-92322 Châtillon FRANCE

Email: [victor.medeau@onera.fr](mailto:victor.medeau@onera.fr), [frederic.laurin@onera.fr](mailto:frederic.laurin@onera.fr), Web Page: <https://www.onera.fr/>

<sup>2</sup>Safran Aircraft Engines, Rond-point René Ravaud, 77550 Moissy-Cramayel FRANCE

Web Page: <https://www.safran-group.com/fr>

<sup>3</sup>ISAE-SUPAERO / Clément Ader Institute, 3 rue Caroline Aigle, 31400 Toulouse

Email: [Frederic.Lachaud@isae-supaero.fr](mailto:Frederic.Lachaud@isae-supaero.fr), Web Page: <http://institut-clement-ader.org/>

**Keywords:** 3D woven composites, energy release rate, size effect, non-linear fracture

## Abstract

The critical energy release rate  $G_C$  was identified on 3D woven carbon/epoxy composites, using CT and SENB specimens. The analysis relied on multiple instrumentation methods to monitor the crack growth and compared several methods for the crack detection and  $G_C$  estimation in order to obtain a robust process. Variation of  $G_C$  with the specimen size and shape was highlighted. A non-linear framework was then proposed to describe fracture propagation in the material, relying on the existence of an internal length. The use of at least two material parameters  $G_f$ , an asymptotic fracture release rate, and  $c_f$ , a characteristic internal length, is necessary to completely describes the variation of the apparent  $G_C$  with the specimen shape and scale. The use of non-linear models introducing internal lengths and controlling the dissipated energy is then investigated to transcribe the experimental results.

## 1. Introduction

The constant rise of 3D woven composite materials use in aeronautics implies a good understanding of their fracture properties, a clear identification of the related parameters and a robust transfer to numerical simulations. These materials exhibit a high level of complexity (heterogeneity, high anisotropy, influence of the local structure) and the methods used to characterize their mechanical behavior must be subjected to a special care.

The characterization of a macro-crack propagation in 3D woven composites with polymeric matrix is a key asset for the future design of aircraft parts. It is usually done through the identification of the critical energy release rate  $G_C$ , which represents the energy released by the structure during the crack propagation divided by the surface area created.

In this work, an experimental study will be performed on both Compact Tension (CT) and Single Edge Notched Beam (SENB) specimens, on a highly unbalanced 3D woven composite (section 2). The special care put on the data analysis will be presented, especially the crack-tracking using several measurement techniques, in order to improve the measurement's reliability (section 2.2). Several methods will be applied to the tests data in order to estimate  $G_C$ , under condition that they don't imply the validity of Linear Elastic Fracture Mechanic (LEFM) or any other spurious assumption (section 0).

In this paper we will study, for this material, the potential variations of the estimated  $G_C$  value depending on the test geometry and size. The influence of the size effect will be investigated by scaling the specimen with in-plane homothetic size factors from 0.75 to 2.5 with respect to the

standard. The difference with the LEFM will be pointed out, which can be explained by the presence within the material of a characteristic length affecting crack propagation [1] and justifies a non-linear framework for the analysis (section 3.1).  $G_C$  thus becomes an apparent value that cannot, by itself, characterise the macro-crack propagation. At least 2 parameters are necessary:  $c_f$  an internal length and  $G_f$  an asymptotic value of  $G_C$  when the size of the specimen is large compared to the internal length of the material.

For further details on the mechanisms responsible for the introduction of an internal length, CT tests carried out in a X-ray tomograph and post-fracture SEM images will be set-up (section 3.2). Two internal lengths characterizing the crack process and induced by the micro-structure of the material will then be introduced and an adapted non-linear model will be presented. The identification of the parameters  $c_f$  and  $G_f$  will accurately describe the experimental results (section 0).

Finally, we will discuss the application of those results into numerical simulations using models introducing internal lengths in order to transcribe the geometry and size effect (section 4).

## 2. Experimental $G_C$ estimation using stress-gradient specimens

### 2.1. Experimental Setup

The tests were carried on a highly unbalanced 3D woven composite provided by Safran Aircraft Engines. The specific characteristics fall under industrial confidentiality, therefore all the results of this study are normalized. This material is manufactured using an epoxy matrix and carbon fibers. The crack will propagate along the warp direction, characterizing the failure of the weft yarns: this facilitates the good execution of the test and especially allows a straight crack path strongly guided by the warp yarns.

The estimation of the critical energy release rate  $G_C$  is performed using stress-gradient specimens exhibiting a stable crack propagation [2]. The compact Tension (CT) and Single Edge Notched Beam (SENB) are used and the configurations for size T1, defined from metallic or ceramic ASTM standards [2], as reported in Figure 1.

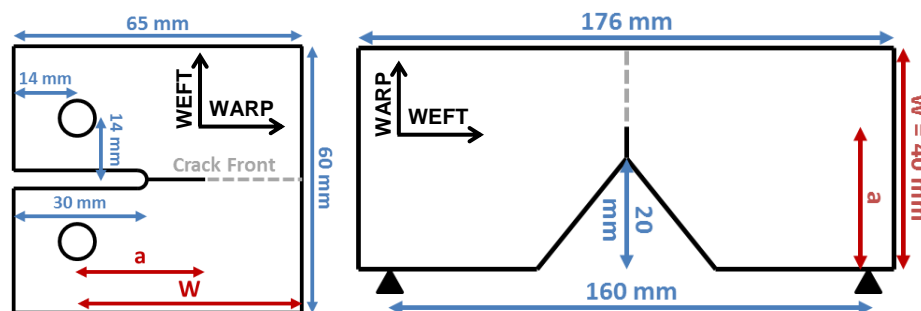


**Figure 1.** CT and SENB standard specimens (Size 1)

Careful consideration should be given regarding the specimen design in order to avoid undesired failure mode:

- The propagation must occur in a quasi-static manner in order to obtain multiple propagation points and thus a sufficient confidence in the experimental results. For this, the pre-crack should be long enough so that  $\partial G/\partial a \leq 0$ , where  $G$  is the energy release rate for a given loading condition and  $a$  the crack length. This condition leads to different pre-crack lengths for the various configurations, presented in the Table 1.
- Undesired compression failure at the back of the specimen [4] should be avoided by using a specimen with large enough dimensions. Indeed, if the crack propagates under a constant value  $G_C$ , the compressive stress at the back of the specimen evolves as  $1/\sqrt{W}$  where  $W$  is the characteristic size of the specimen [5]: the bigger the specimen, the later compressive damage may occur.

- On the other hand, the thickness  $t$  of the specimen should be sufficient compared to the  $W$  in order to avoid failure by buckling during the CT tests, with is prevented here by the use of specimens with a thickness  $t$  equals to 8mm.

Following those requirements, the various configurations of CT and SENB specimens tested are presented in Table 1.

**Table 1.** Summary of the stress-gradient specimens tested and associated instrumentation

Specimen Type	Size	W [mm]	Pre-crack [mm]	Quantity	DIC	OT	IRT	$\mu$ -T
CT	T0.75	38.2mm	4mm	2	x	x		IS
	T1	51mm	5mm	2	x	x		PT
	T1.5	76.5mm	6mm	2	x	x	x	PT
	T2	102mm	8mm	2	x	x	x	PT
	T2.5	127.5mm	10mm	3	x	x		PT
SENB	T1	40mm	7mm	3	x	x		PT

## 2.2. Crack Length Measurement

Several instrumentation methods were used to follow the crack tip position  $a$ , as this value is a key parameter for the estimation of the energy release rate. The tests are instrumented using Digital Images Correlation (DIC), Optical Tracking (OT), passive Infra-Red Thermography (IRT) and X-ray tomography ( $\mu$ -T), either Post-Test (PT) or In Situ (IS). The data from those instrumentations are compared in order to avoid any dependency to a specific method and consolidate the results, as they each rely on a specific kind of information : visible macro-crack at the surface (OT) or inside the specimen ( $\mu$ -T), mechanical displacement fields (DIC) or thermal heating at the propagation points (IRT).

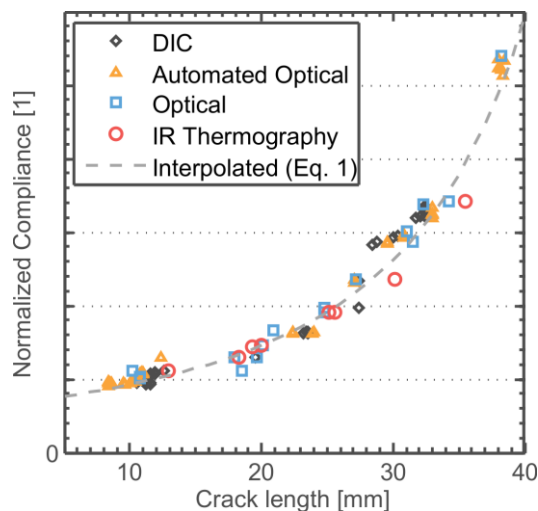


**Figure 2.** Comparison of the crack length measurement

The several instrumentation analysis methods have been automated and the results are presented in Figure 2. The deviation observed between the methods is of the same order of magnitude than differences observed on each side of the specimen and remains small in comparison to the total length propagation. More importantly, as only the crack length variation is used for the  $G_C$  estimation methods later presented (see section 0), no impact is subsequently observed on the resulting energy release rate estimation. For the present study, fast automated methods available at any time, i.e. the automatic optical tracking and DIC tracking, have been used and confronted on each side to obtain a reliable measurement.

## 2.3. $G_C$ estimation

The characterization of fracture propagation is usually done via an energetic approach, which tries to estimate the critical energy release rate  $G_C$ . In the general framework of LEFM,  $G_C$  does not depend on the geometry or the crack length and is assumed to be a material property. The variation of  $G_C$  with the geometry and size is here investigated through the analysis of the different tested configurations, especially the in-plane homothetic sizing of the CT specimens.

Several methods for estimating the critical energy release rate are available in the literature [2], [3]. Two methods are selected here based on the fact that they don't rely on any unfounded assumption in the context of 3D woven composite testing.

**Area Method:** It consists in a direct estimation of the elastic energy variation between two propagation points over the crack surface created.

$$G_c = \frac{P_1 d_2 - P_2 d_1}{2 t \Delta a} \quad (1)$$

with  $P_i$  and  $d_i$  the load and displacement at a propagation time  $i$ ,  $t$  the thickness and  $a$  the crack length.

**Modified Compliance Method (MCM):** The energy change can also be obtained in a continuous manner by using the change in the compliance with the crack length evolution:

$$G_c = \frac{P_c^2 dC}{2t da} = \frac{P_c^2 dC}{2tW dx} \quad (2)$$

with  $C = d/P$  the compliance and  $x = a/W$  the normalized crack position. It requires interpolating the compliance at each measured crack length in order to compute the derivate. The interpolating function is chosen as:

$$C(x) = \frac{C_0}{(x_m - x)^p} \quad (3)$$

which is based on by the evolution of the compliance under LFM assumptions [6], so that parameters are expected to be  $x_m \approx 1$  and  $p \approx 2$ . Those two methods are in good agreement and don't introduce any bias in the results. On the contrary, the VCCT method or methods using interpolation of the stress intensity factors were excluded. These methods are in fact conducted under LFM assumptions: they use numerical simulations assuming that the material behavior stays elastic around the crack.

A variation with the size and geometry of the estimated  $G_c$  value is highlighted in Figure 3. It invalidates the use of the general LFM framework for describing the crack propagation in 3D woven composite, although this phenomenon isn't usually exhibited in laminated composites. An adapted framework describing the evolution of the apparent  $G_c$  value with the shape and size of the specimen is thus needed, as  $G_c$  can no longer be considered as a material property.

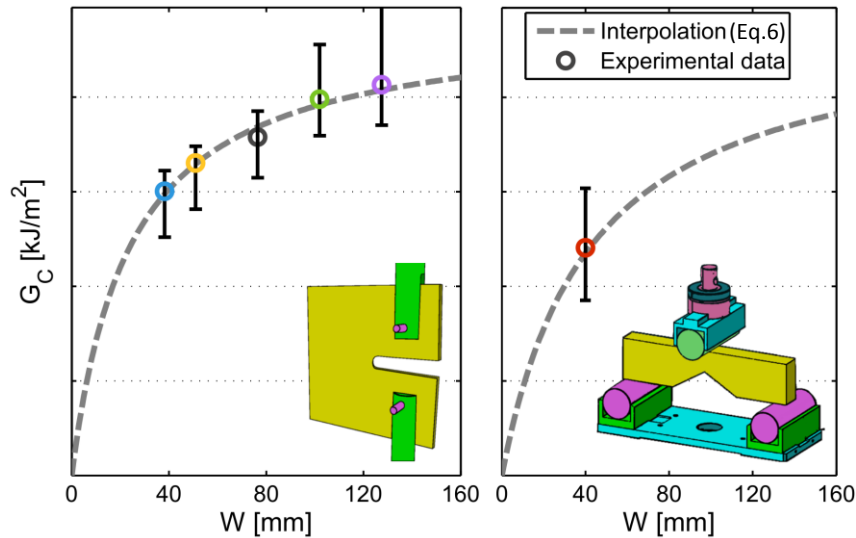


**Figure 3.** Experimental results of the  $G_c$  estimations obtained from CT and SENB specimens

### 3. Non-linear framework for crack propagation

#### 3.1. Apparent $G_C$ value in presence of size and geometry effect

The size effect in fracture has already been studied by Bazant, especially in the case of concrete [1]. The scaling laws when studying homothetic specimens can in the general case, in presence of material internal lengths guided by the meso-structure and affecting the crack propagation, be expressed through energetic considerations as [1] :

$$G_C = \frac{G_f}{1 + W_0/W} \quad (4)$$

where  $G_f$  is the asymptotic value of  $G_C$  : when the specimen size is large enough it identifies as the LEFM value.  $W_0$  is a transition size of the specimen from a crack propagation driven by local mechanisms to a propagation under brittle conditions and described by the LEFM theory.  $W_0$  depends on an internal length  $c_f$ , considered as a material value. The mechanisms responsible for this behavior must be exhibited in order to explicit the dependency of  $G_C$  to  $c_f$  and to compare the values obtained on specimens with different geometrical singularities.

#### 3.2. Investigation of the crack mechanisms

For this purpose, complementary tests are performed on the same 3D woven material:

- Scanning Electron Microscope (SEM) views of the crack profile are obtained from fractured specimens to investigate the distribution of the pull-out length of the yarns on both sides of the average crack surface. This distribution does not seem to vary with the geometry or the size of the specimen and happens over a characteristic length of a few millimeters (see Figure 5. ). This introduces a notion of crack width, which is a compatible mechanism for the evolution of the apparent  $G_C$  value.
- In-situ X-ray tomographic tests are also performed on CT specimens using a special assembly designed to carry out the CT tests inside the tomograph chamber without interfering with the X-rays. The progressive failure of the fiber inside the yarn can be observed, occurring over the range of two columns of waft yarns: as showed in Figure 4. A sectional cut through the yarn column currently transmitting loads shows that some of the yarns in that column are already cracked while others appear to be intact. This introduces, along with the numerous transverse cracks and inter-yarn debonding observed, a notion of process zone along which failure happens in a progressive manner. The characteristic size of this process zone is of the same order of magnitude as the length between two weaving columns.

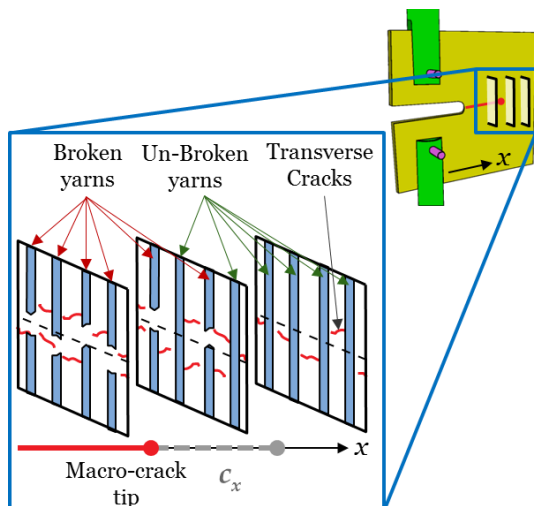


**Figure 4.** Diagram of the crack built-up obtained from in-situ X-ray tomography

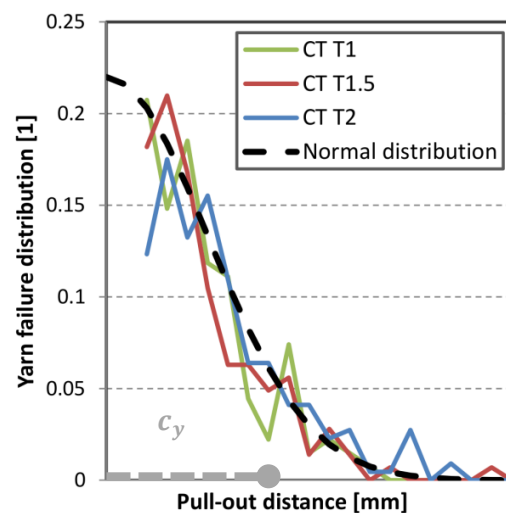


**Figure 5.** Distribution of the yarn pull-out distance for different CT specimens

The identification of those mechanisms can explain the evolution of  $G_C$  with the geometry and size of the specimen and calls for an adapted fracture framework which introduces two internal length:  $c_x$ , a process-zone length introduced along the crack path and  $c_y$ , a crack width perpendicular to the crack surface.

### 3.3. Equivalent configuration using two internal lengths

Such a framework can be introduced by considering equivalent linear elastic (LE) configurations (see Figure 6. ). In this approach, the real configuration of the crack, which presents a non-linear area around the macroscopically observed crack, is approximated by an equivalent elastic configuration that leads to identical mechanical fields away from the crack and identical load/displacement curves. This configuration is obtained by introducing a shift  $c_x$  between the observed macro-crack and the equivalent crack and by giving a width  $c_y$  to the crack. Both  $c_x$  and  $c_y$  are assumed to be material properties which do not vary with the crack propagation or the geometry.

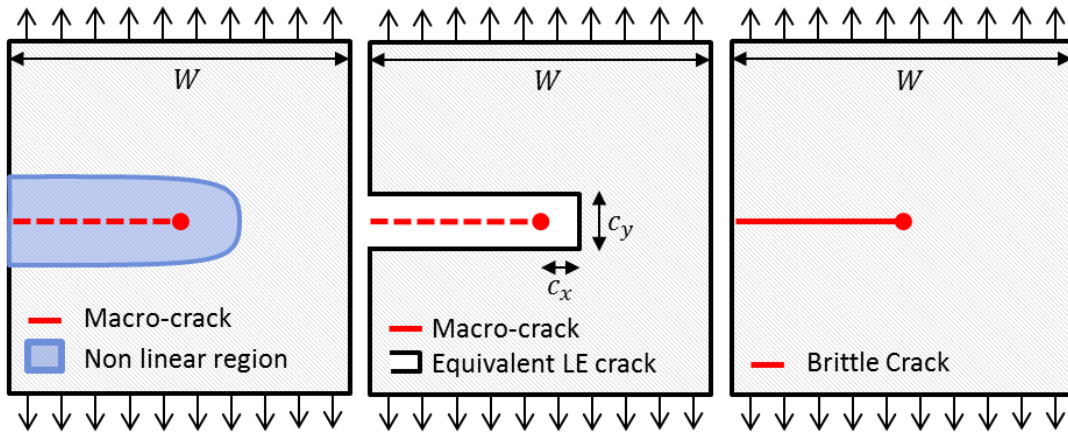


**Figure 6.** Real configuration, Equivalent Elastic configuration and Brittle configuration

For brittle cracks, the energy release rate can be generally expressed in the form of [1] :

$$\text{Brittle configuration : } G_C = \frac{P_C^2}{WE'} g(x) = \frac{P_C^2}{WE'} g(x, 0, 0, \dots) \quad (5)$$

where  $E'$  is an equivalent modulus of the material and  $g$  a dimensionless function that only depends on the shape of the stress fields around the crack tip through the normalized position  $x$  of the crack. This configuration only takes into account the macro-crack surface and neglects the presence of non-linearities around the crack tip. It fits the usual definition of  $G_C$  defined by the dissipated energy over the created crack surface and applied in section 2.

The brittle configuration can be considered as a particular case of a general framework with the others non-linear parameters taken equal to zero (Eq. 5). The equivalent LE configuration allows a more accurate description of the real fracture process and can introduce the internal lengths  $c_x$  and  $c_y$  through dimensionless arguments:

$$\text{Equivalent LE configuration : } G_f = \frac{P_C^2}{WE'} g\left(x, \frac{c_x}{W}, \frac{c_y}{W}\right) = \frac{P_C^2}{WE'} g\left(x + \frac{c_x}{W}, \frac{c_y}{W}\right) \quad (6)$$

Here,  $g$  takes two parameters:  $c_x$  is introduced via a shifting of the crack tip position  $x$ . The fracture energy release rate  $G_f$  thus defined takes into account all the failure phenomena and can be taken as a material property. The evolution of the apparent energy release rate  $G_C$  is then obtained by:

$$G_C = \frac{G_f g(x, 0)}{g\left(x + \frac{c_x}{W}, \frac{c_y}{W}\right)} \cong \frac{G_f}{1 + \frac{\partial_{c_x} g(x)}{g(x)} \frac{c_x}{W} + \frac{\partial_{c_y} g(x)}{g(x)} \frac{c_y}{W}} \quad (7)$$

which is similar to the Eq. 4 for  $W_0(c_x, c_y) = \partial_{c_x}g(x)/g(x)c_x + \partial_{c_y}g(x)/g(x)c_y$ . The function  $g$  and its derivatives over the internal lengths can be obtained from linear elastic simulations, by varying the position and width of the crack inside a given structure (see Figure 7. ), and can be compared to the values given in crack hand books [6] for the derivative along the  $x$  value.

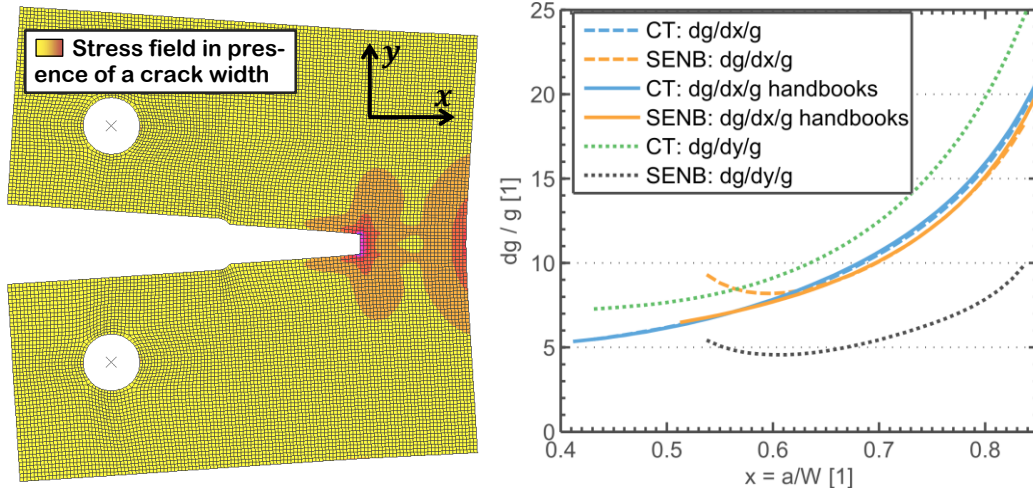


**Figure 7.** Numerical determination of the  $g$  function for CT and SENB specimens

Once the  $g$  functions have been determined for CT and SENB specimens, the identification of the material parameters  $G_f$ ,  $c_x$  and  $c_y$  accurately describes the evolution of the apparent  $G_C$  estimated during the experimental campaign (see the dashed line on Figure 3. ). It explains the increasing value of  $G_C$  with the specimen size and the differences between CT and SENB specimens. The values of  $c_x$  and  $c_y$  are in good agreement with the order of magnitude of the phenomena observed in section 3.2.

In equation 7, the evolution of  $G_C$  is determined by:

- Parameters specific to the studied configuration, which need to be modified for every test:  $W, x, g(x)$  and its derivatives;
- Parameters specific to the material, which are identified once for all:  $G_f, c_x$  and  $c_y$ .

This framework can be used to predict the  $G_C$  value for any given structure once the  $g$  function has been determined through linear elastic simulation. Note that this model can also be extended to any number of internal lengths as long as their influence on the equivalent elastic configuration is explained.

#### 4. Use in numerical simulations

When trying to transcribe the crack propagation in 3D woven composites, the experimental results lead to the use of fracture models introducing internal lengths and in which the energy can be controlled in order to obtain the same size and geometry effects.

Numerical simulations of the behavior of composites are usually performed using continuous damage models [7]. Those models introduce internal variables transcribing the progressive failure of the fiber and offer an adapted framework for describing the transition from diffuse damage mechanisms to the apparition of a macro-crack, without having to pre-determine the crack path.

However, it has been demonstrated that the stress-strain softening introduced to account for the fiber failure variables leads to ill-defined problems which compromise the simulations [8]. Moreover, those models don't introduce internal lengths and don't exhibit the size effect observed during the tests.

Thus, the focus should be put on gradient or non-local damage models, which both make up for the ill-posed problem and introduce internal lengths characterizing the fiber yarns failure. Several approaches can be found in the literature (integral non-local [9], gradient non-local [10], phase field [11]). The practical choice should be guided by the fact that the model leads to an evolution of the apparent critical release rate  $G_C$  with the specimen size and geometry which match the one met in the



experimental campaign.

## 5. Conclusions

An experimental characterization of the crack propagation was performed on 3D woven composites, using CT and SENB specimens. A special care was put on the crack length measurement and critical energy release rate  $G_C$  estimation in order to assure a robust methodology. Several configurations were tested in order to determine a potential effect of the specimen size and geometry. The results show a strong evolution of the apparent measured  $G_C$ , which in particular increases with the size of a specimen until  $G_C$  reaches an asymptotic value, when the effects of the micro-structure is of a small enough scale compared to the mechanical fields.

This result compromises the use of the Linear Elastic Fracture Mechanic to describe the crack propagation in 3D woven composites and necessitates the introduction of internal lengths influencing the crack formation. The investigation of the cracking process highlighted the presence of two characteristic material length linked to the micro-structure: a shifting  $c_x$  along the crack axis due to a process-zone ahead of the macro-crack tip and a crack width  $c_y$  transcribed by a yarn failure and pull-out distributed across the main crack surface.

A non-linear fracture model was then proposed taking into account the influence of those two mechanisms on the apparent  $G_C$  value at the macroscopic scale. The identification of the internal lengths  $c_x$  and  $c_y$  are consistent with the characteristic size of the phenomena observed in the tests.

Those results guide the choice of numerical models to describe the crack propagation in 3D woven composite: internal lengths should be introduced in those models and the dissipated energy must be controlled in order to exhibit the same size and geometry effects than have been highlighted in the experimental campaign. Non-local continuous damage models could be used.

## References

- [1] Z.P. Bazant, J. Planas. *Fracture and Size Effect in Concrete and Other Quasibrittle Materials*. CRC Press, 1997
- [2] ASTM. *Standard Test Method for Plane-Strain Fracture Toughness of Metallic Materials* (No. E399-90). ASTM International, 1997.
- [3] M.J. Laffan, S.T. Pinho, P. Robinson, L. Iannucci. *Measurement of the in situ ply fracture toughness associated with mode I fibre tensile failure in FRP. Part I: Data reduction*. Composites Science and Technology, 70:606–613, 2010.
- [4] A. Ortega, P. Maimi, E.V. Gonzalez, L. Ripoll. *Compact tension specimen for orthotropic materials*. Composites Part A: Applied Science and Manufacturing, 63: 85–93, 2014
- [5] Z.P. Bažant. *Scaling Laws in Mechanics of Failure*. Journal of Engineering Mechanics, 119 :1828–1844, 1993.
- [6] H. Tada, P.C. Paris, G.R. Irwin. *The Stress Analysis of Cracks Handbook, Third Edition*. ASME, 2000.
- [7] A. Hurmane, A. Mavel, P. Paulmier, F. Laurin, 2016. *Combined experimental and modelling approaches for strength analysis of 3D woven composites: from elementary coupons to complex aeronautical structures*. AerospaceLab Journal, 1-11, 2016
- [8] R. De Borst, L.J. Sluys, H.B. Muhlhaus, J. Pamin. *Fundamental issues in finite element analyses of localization of deformation*. Engineering Computations, 10(2):99-121, 1993.
- [9] G. Pijaudier-Cabot, Z.P. Bažant. *Nonlocal Damage Theory*. Journal of Engineering Mechanics, 113:1512–1533, 1987
- [10] R.H.J. Peerlings, R. De Borst, W. Brekelmans, J.H.P. De Vree. *Gradient Enhanced Damage for Quasi-Brittle Materials*. Int. J. Numer. Meth. Engng., 39:3391–3403, 1996
- [11] C. Miehe, D. Kienle, F. Aldakheel, S. Teichtmeister. *Phase field modeling of fracture in porous plasticity: A variational gradient-extended Eulerian framework for the macroscopic analysis of ductile failure*. Computer Methods in Applied Mechanics and Engineering, 312: 3–50, 2016.